N93-28269

THERMAL EXPANSION BEHAVIOR OF LDEF METAL MATRIX COMPOSITES

Tuyen D. Le
Mechanics and Materials Technology Center
The Aerospace Corporation
P.O. Box 92957
Los Angeles, CA 90009
Phone: 310/336-7864, Fax: 310/336-5846

Gary.L. Steckel
Mechanics and Materials Technology Center
The Aerospace Corporation
P.O. Box 92957
Los Angeles, CA 90009
Phone: 310/336-7116, Fax: 310/336-7055

SUMMARY

The thermal expansion behavior of LDEF metal matrix composite materials was studied by (1) analyzing the flight data that was recorded on orbit to determine the effects of orbital time and heating/cooling rates on the performance of the composite materials, and (2) characterizing and comparing the thermal expansion behavior of post-flight LDEF and lab-control samples. The flight data revealed that structures in space are subjected to non-uniform temperature distributions, and thermal conductivity of a material is an important factor in establishing a uniform temperature distribution and avoiding thermal distortion. The flight and laboratory data showed that both Gr/Al and Gr/Mg composites were stabilized after prolonged thermal cycling on orbit. However, Gr/Al composites showed more stable thermal expansion behavior than Gr/Mg composites and offer advantages for space structures particularly where very tight thermal stability requirements in addition to high material performance must be met. .

INTRODUCTION

The Advanced Composites Experiment is a sub-experiment of LDEF Experiment M0003, "Space Environmental Effects on Spacecraft Materials." The sub-experiment is a joint effort between government and industry, with Air Force Wright Laboratory, Flight Dynamics Laboratory, and the Aerospace Corporation, Mechanics & Materials Technology Center acting as experimenters.

In our first paper, presented at The First LDEF Post-Retrieval Symposium, we examined the microstructure and discussed the effects of atomic oxygen erosion, micrometeoroid bombardment, surface contamination on physical morphology, and surface damage of composite materials (Ref. 1). Besides these factors, in low earth orbit, the materials are also subjected to thermal cycling effects due to alternating eclipse and sun exposure. The materials experience transient heating/cooling in addition to thermal gradients. The effects of this environment on the thermal expansion behavior of composite materials needed to be characterized and documented. Therefore, the present analysis evaluates the thermal expansion behavior of post-flight composite materials compared with lab-control samples. In this analysis, temperature change vs. time, dimensional change vs. temperature, coefficients of thermal expansion (CTE), and thermal hysteresis are considered in predicting the dimensional stability experienced by the metal matrix composite materials in the space environment.

The analysis was done in two parts: (1) analysis of the flight data that was recorded on orbit to determine the effects of orbital time and heating/cooling rates on the performance of the composite materials, and (2) the characterization and comparison of the thermal expansion behavior of post-flight LDEF and lab-control samples. This study, combined with the results previously reported (Ref. 1), completes a full evaluation of all factors affecting composite materials in the LDEF space environment. This allows us to evaluate possible synergistic effects of long term space exposure that cannot be studied on earth.

MATERIALS AND EXPERIMENTAL PROCEDURE

The experiment includes a wide variety of metal matrix composites (MMC). The materials selected for this study are shown in Table I. The "Material Description" column first specifies the type of fibers and then the materials for the matrices and face sheets. The MMC's are primarily continuous graphite fiber-reinforced aluminum and magnesium alloys. They are either single-ply or multi-ply composites with different ply angles. In each group, typical procedures were followed to produce five (5) sets of samples: leading-edge (LE) exposures, trailing-edge (TE) exposures, LE controls, TE controls, and lab-control samples. The lab-control samples were stored in vacuum on earth. The locations of flight samples on LDEF were Bay D, Row 4 on the TE and Bay D, Row 7 on the LE. It is worth noting here that the LDEF samples were mounted such that there was no clamping force on them, i.e. the samples were free to expand or contract in their slots. The sample cassettes were thermally decoupled from the LDEF to minimize effects of the structure on the temperature excursions. The LE and TE controls were mounted on the back side of cassettes, facing inward, not directly exposed to the space environment. However, they were expected to be subjected to thermal excursions similar to those experienced by the exposed samples. The samples were 3.5 in. long X 0.5 in. wide X 0.031 in. thick strips. One or more samples from the top two classes of Gr/Al composites listed in Table I and the MG3-MG6 group of Gr/Mg composites were instrumented with thermistors and strain gages (SG) to monitor the thermal cycles and thermal strains during orbiting. It should be noted that the SG and thermistors were only mounted on the back side of LE and TE exposures, and not directly exposed to the thermal radiation in space. This was done to avoid any possible damage caused by atomic oxygen erosion, UV radiation, or micrometeoroid bombardment on these sensors. The strain gages were mounted to measure the change in dimension along the direction parallel to the fibers. The data acquisition system was set up to record temperature and strains during the duration of an orbit once every 107 hrs. (approximately 78 orbits.) Data were collected every three minutes during the selected orbit. For the record, the first set of data was collected after approximately 44 hours on orbit, and the last set was recorded after approximately 14 months into the flight. No data were recorded during the unplanned final 4.5 years of the mission.

In the flight data analysis, typical thermal expansion curves were selected at the beginning, middle, and the end of the recording time. These durations are approximately 40, 5K, and 10K hours (1, 208, 416 days) after being placed in orbit. These curves were all selected over the same range of temperature for the purpose of comparisons. The thermal cycles of each type of material were also analyzed to determine the heating and cooling rates.

The absolute values of linear thermal expansion in composite materials are extremely small, particularly in the direction parallel to the fibers. This requires the use of a highly specialized, sensitive, stable, high resolution apparatus like a laser interferometer. In this study, the Michelson Laser Interferometer of The Aerospace Corporation was used to characterize the thermal behavior of LDEF post-flight and lab-control samples. This technique provides in-situ, direct, and continuous measurements of thermal expansion/contraction through a thermal cycle without recourse to a comparative standard. It also allows very small changes in dimension (on the order of 1μ-strain or less) to be resolved. This technique has been described in detail elsewhere (Refs. 2, 3). Before mounting on the interferometer, the ends of each strip sample were slightly ground to a dome shape. This was done to avoid the effects of thermal distortion in the face sheet at the ends of the sample that could cause error in the measurements. A chromel-alumel thermocouple was mounted on each side of the sample to monitor the temperature change. In all cases, thermal cycling was carried out by heating the sample first from room temperature (RT) to the hot end of the cycle, and then cooling down to the cold end and heating back up to RT. The heating/cooling rate was limited to ~1°C/min. to ensure thermal equilibrium throughout the sample. Again, for the purpose of comparison with the flight data, the samples were thermally cycled over the same range of temperature that was derived from the flight data analysis.

RESULTS AND DISCUSSION

In this section, the flight data analyses are presented first, followed by the results obtained using the laser interferometer. It should be noted that all thermal expansion curves are plotted on coordinates of the same dimensions to provide consistency for comparisons.

Gr/Al Composites

Figures 1 and 2 show the change in dimension vs. temperature of P55/6061/6061 and GY70/201/2024 composites mounted on LE and TE respectively. Figure 1 shows the thermal expansion behavior of P55/6061/6061 composites after 40, 5K, and 10K hours in orbit. It is clearly seen that generally the behavior was fairly linear with only a small hysteresis. During the entire duration of orbiting or at least for the first 10 thousand hours (approximately 6,150 cycles), the behavior of this material showed little change. The curves consistently conformed to the same shape with the same total change of length. A similar behavior was observed for the GY70/201/2024 composites, except that this material showed more thermal hysteresis, particularly in the TE sample, Fig. 2. However, in all cases, the total changes in dimension and the slopes remained constant during the entire time of recording. When the LE and TE curves for either of these Gr/Al composites were compared, it was noted that the total dimensional changes in the TE samples were smaller than for the LE samples, even though the temperature span was about the same.

The thermal cycles of LE and TE Gr/Al samples were also analyzed. The results showed a consistent shape of the temperature/time plots for either LE or TE for both types of Gr/Al composites. The typical cycles are shown in Figs. 3(a) and (b) for the GY70/201/2024 composites. The only differences between samples were the starting point and the end of the cycle that obviously depended on when the data were recorded. In both cases, it is seen that the samples did not have constant heating/cooling rates throughout a cycle. As seen in Fig. 3(a), the samples on the LE heated very rapidly at a rate of ~15°F/min. when the heating cycle started. The heating rate slowed down when the temperature approached the hot end. Initial cooling was just as fast as initial heating, but again the rate slowed down to ~ 1-2°F/min. when approaching the cold end. However, an important point to be noted here is that the heating and cooling rates were twice as high in the LE than TE samples. It is also noted that the hot end of the TE thermal cycle was sharper than for the LE; the dwell time for the transition from heating to cooling of the TE samples was much less than for the LE, causing an abrupt, sharp drop in temperature on the TE.

Figure 4 shows the change in dimension vs. temperature of single-ply P100/EZ33A/AZ31B mounted on the LE and TE, respectively. These curves again were plotted for thermal cycles selected at the beginning, middle, and the end of the recording time. It is clearly seen that the thermal behavior plotted from flight data are completely different from the normal response for this material. Instead of expanding and contracting upon heating and cooling as shown for the Gr/Al composites, these materials expanded and then slowly contracted with increasing temperature and vice versa upon cooling, forming convex curves. This anomalous behavior was further investigated and will be explained later when the change in temperature and the corresponding change in dimension vs. time for each individual curve are examined.

In comparing the LE and TE samples, the thermal behavior was very similar in that the curves followed the same pattern. The dimensional change was observed to continually change as a function of the number of thermal cycles. The curves shifted upward indicating that the samples were getting longer with time until stability was attained. Significant shifting occurred in the first five thousand hours of flight, but minimal shifting occurred between the 5K and 10K hour curves. It should be noted that during the first 40 hours of flight after the LDEF was released, no data were recorded. Therefore, for the first 27 cycles, it is possible that the behavior of the samples was very unstable. Apparently the dimensions were reduced from the initial SG reading of 0.0 μ-strain to a minimal value during the first few cycles and then increased with additional cycles until the final, stable dimensions were attained. It can be seen in Fig. 4 for the TE sample that the data recorded at 40 hrs. shows more scatter as compared to the LE, indicating that the TE sample was more unstable after 40 hrs of flight. The 5K and 10K hour curves are smooth, and the data fall consistently along the same path. This indicates that after a certain number of thermal cycles, the Gr/Mg composites stabilized and behaved quite consistently.

Figure 5 shows a typical thermal cycle and the corresponding dimensional change for the Gr/Al composites plotted vs. time. This plot shows the normal behavior of Gr/Al composites which expand and contract with heating and cooling throughout the cycle. The rates of change in dimension were consistent with the rates of change of temperature. When the same curves were plotted for Gr/Mg composites, anomalous behavior was observed as shown in Fig. 6 . As the cycle started, temperature increased slowly and the sample expanded as expected. However, as the heating rate rapidly increased, the sample contracted instead of expanding. The sample kept contracting until the hot end point was reached. Upon cooling, at first the temperature dropped very rapidly and the sample expanded instead of contracting. As the cooling rate slowed down, the sample started contracting as originally expected. Two factors are used in explaining this unusual phenomenon. First, in the original set-up of the experiment, the SG and thermistors were mounted on the back side of the sample. They were not directly exposed to radiation, which is the heating source. Second, the thermal conductivity of Gr/Al composites is significantly greater than Gr/Mg due to the much higher matrix conductivity of the Al matrix alloy compared to the Mg alloy (1104 vs. 408 Btu-in/ hr. ft °F). When the exposed surface of the Gr/Mg samples was heated or cooled slowly (in this case at the rate of 1.5°F/min. or less), thermal equilibrium was maintained throughout the sample leading to normal behavior. However, when just leaving or entering the shadow, the samples were heated or cooled at a much faster rate (10°F/min.). Due to the low thermal conductivity of the Gr/Mg, a steep thermal gradient existed through the thickness. A larger temperature gradient existed between exposed front-surface and back-side surface in the Gr/Mg composite materials than for Gr/Al. Upon heating, the exposed surface was therefore much hotter and consequently expanded faster than the back surface, causing sample bending and inducing compression in the back surface leading to negative SG readings. These bending deformations give the erroneous indication that the sample has a negative CTE. Similar arguments apply for the fast cooling condition, the exposed surface cooled faster making the sample bend the other way. This time the bending induced tension on the back side and led to expanding readings by the SG, again implying that the sample had a negative CTE. Consequently, the anomalous behavior of the Gr/Mg composites resulted from the nature of the space exposure and the experiment design and was not an inherent characteristic of the materials themselves. The temperature versus time plots for the Gr/Mg composites mounted on LE and TE showed the same features as observed for Gr/Al composites, except that the heating and cooling rates were higher than for Gr/Al (20 and 10°F/min. as compared to 15 and 7°F/min.). This again might be attributed to the combined effects of low thermal conductivity and differences in solar absorptance and emissivity of Gr/Mg composites.

From the results of flight data analysis, it is clearly shown that in a space environment, the temperature distribution in a structure is not uniform. Nonuniform temperatures arise from radiant heating on one side of a structure as typically occurs in a geostationary satellite or by transient heating/cooling as in the LDEF structure placed in a day-night low earth orbit with alternating eclipse and sun exposure. Depending on the location, as in this case LE or TE, materials are subjected to widely different temperature ranges and heating/cooling rates. The disparity of the temperature range and rates of heating/cooling lead to a differential total change in dimensions that could eventually lead to thermal distortion. In low thermal conductivity materials like Gr/Mg or Gr/Epoxy composites, the thermal gradient effects on distortion are more severe. Therefore, besides the thermal expansion behavior (CTE and thermal hysteresis), thermal conductivity must be considered in predicting the structural stability of a material in the space environment.

Laser Interferometer Data Analysis

Gr/Al Composites

The flight samples with mounted strain gages and thermistors selected for flight data analysis were subsequently used in the lab to characterize the post-flight thermal expansion behavior. These samples as well as lab-control samples of the same material were characterized with the laser interferometer over the same ranges of temperature derived from flight data. The thermal expansion curves of single-ply GY70/201/2024 are shown in Figs. 7 to 10. Fig. 7 shows the comparison between thermal expansion curves of LE and TE samples. The LE curve illustrates linear, stable behavior with zero hysteresis. The upper half of the TE curve did not retrace along the same path upon cooling resulting in a residual thermal strain of about 20 μ-strain that caused a permanent offset when the cycle was completed at RT. The offset that occurred in the TE samples is not readily explainable. However, the overall behavior was linear and stable with small hysteresis. Fig. 8 compares the thermal expansion curve of a lab-control sample with the LE sample. In the lab-control sample, the change in specimen length upon heating from RT to the hot end of the cycle was not recovered on cooling back to RT, i.e., upon cooling the dimensional change did not retrace the same path as heating. Further cooling from RT to the cold end and heating back up to RT also did not result in recovery of the total length change. A residual thermal strain was induced such that a thermal strain hysteresis was formed with permanent offset at RT of ~ 10 μ-strain. The lab-control sample shows a small, open thermal hysteresis loop of about 20 μ-strain wide. The results indicated that after a certain number of thermal cycles in space, strain hardening in the matrix stabilized the composites, reducing thermal hysteresis for subsequent thermal cycles.

The P55/6061/6061 composites showed basically the same behavior; therefore, the results are not shown here. The post-flight samples behaved elastically over the entire temperature range with no hysteresis. The lab-control sample behavior was stable and linear with a very small hysteresis of about 5 μ-strain. The very small hysteresis demonstrates that the high yield strength of 6061 matrix probably delays the plasticity of the matrix to broader temperature ranges than encountered in low earth orbits. The average CTE for all Gr/Al composite samples determined over the entire temperature range is listed in Table II. It may be seen that the CTE of both composite materials was apparently unaffected by the extended space exposure. These results indicate that the LDEF space environment has little effect on the thermal behavior of Gr/Al. Thermal cycling in orbit stabilized the Gr/Al composites, eliminating thermal hysteresis after a number of cycles.

In order to simulate the thermal cycling conditions experienced by a satellite in a geosynchronous orbit, additional measurements were made on the lab-control and flight samples over the temperature range of ±250°F. These measurements were performed at Composite Optics, Inc., San Diego, CA. The results are shown in Figs. 9 to 12. In these experiments, two continuous thermal cycles were performed. For each cycle, the samples were first cooled from RT to -250°F, heated up to + 250°F, and then cooled to RT. As shown in Fig. 9, the behavior of the lab-control sample was not as linear as in the narrower temperature range. At temperatures near both extremes, the behavior deviated from linearity due to the plasticity in the matrix, leading to the formation of an open hysteresis loop. It is noted that the hysteresis of the second cycle is larger than that of the first cycle (100 μ-strain and 50 μ-strain respectively). It is not well understood why upon cooling for the second cycle, the matrix yielded at a higher temperature than for the first cycle leading to the formation of a larger loop. From our experience, in the first few cycles, the behavior of composite materials can be quite erratic and unpredictable, until the materials stabilize and behave more predictably. As shown in Fig 10, the LE sample was cycled over the same temperature range. It is seen that for both cycles, the flight sample expanded and contracted along the same linear path and was hysteresis-free. This indicates that after the excessive thermal cycling on LDEF, the material was very stable even over a much wider temperature range.

The thermal expansion behavior of the 4-ply/±20° lab-control and LE samples are shown in Figs. 11 and 12. Both samples showed non-linear response with a larger thermal hysteresis loop for the second cycle. The overall response shown is characteristic of angle ply laminates. The average CTE is lower compared to unidirectional, single ply composites because of the interaction between plies and a higher volume fraction of fibers in the 4-ply composites. However, the hysteresis loop is wider due to the existence of interply stresses. After extensive thermal cycling in orbit, the CTE of the post flight sample is about the same as of the lab-control sample. The thermal hysteresis of the post-flight sample is slightly larger (150 to 120 μ-strain). Additional post-flight measurements need to be made on another LE or TE sample over the LDEF temperature range to better indicate the effect of prolonged thermal cycling on the hysteresis for this composite. However, it can be deduced from Figs. 11 and 12 that, over the LDEF temperature range, the thermal behavior would be linear with only a small thermal hysteresis loop. Microstructure examination of both lab-control and post-flight samples revealed no cracking, delamination, or debonding.

Gr/Mg Composites

Figure 13 shows thermal behavior of P100/EZ33A/AZ31B post-flight and lab-control samples. It is clearly seen that the lab-control sample was very unstable. The behavior was non-linear with a large residual thermal strain at RT of ~ 280 μ-strain. The large residual strain of the material in the as-fabricated condition is typical of the MMC, and is caused by yielding of the matrix, in this case, upon cooling to the cold end of the cycle. The composite behavior near the cold end of the cycle was dominated by the expansion of the fibers causing yielding in the matrix. This leads to an increase in dimension and consequently an open loop with large permanent offset at RT. The thermal expansion behavior of post-flight samples showed that the amount of permanent offset and the magnitude of thermal hysteresis over the temperature range decreased remarkably after thermal cycling. The implication of the results is that extensive thermal cycling had a large effect on stabilizing the behavior of these materials. However, the thermal expansion behavior remained non-linear and the thermal hysteresis could not be cycled out as in the case of Gr/Al composites even after nearly 30K cycles. These data indicate that the EZ33A Mg alloy, unlike the high strength 6061 and 201 Al alloys, was not effectively strain-hardened by thermal cycling, which would have increased the yield strength and minimized strain hysteresis over the LDEF temperature range. It should be noted however that the total dimensional change and average CTE of the Gr/Mg composites are smaller than those of the Gr/Al composites. This is due to the low elastic modulus of the Mg alloys (6.5 Msi) and the high modulus, low CTE P100 fiber. The CTEs are near-zero and similar for both LE and TE samples within the error range of the experiment.

It should be noted that P100/EZ33A/AZ31B composites are an obsolete system. During the initial sample preparation stage for LDEF these were the only Gr/Mg composites being produced. It was later learned that P100/EZ33A/AZ31B composites had inherently low strength properties due to interaction between the rare earth elements in the EZ33A matrix alloy and the P100 fibers. This interaction may also affect the matrix and limit its work hardening so that hysteresis in the thermal expansion curves cannot be eliminated. Shortly before the M0003 trays were shipped to NASA before launch, several P100/EZ33A/AZ31B composites were replaced by P100/AZ91C/AZ61A Gr/Mg composites. This system subsequently became the most commonly produced Gr/Mg composites. None of the P100/AZ91C/AZ61A composites were instrumented with thermistors or strain gages because of their late addition to the experiment.

The Gr/Mg composite materials were also tested over a wider range of temperatures to simulate the conditions of higher orbits. The results of LE and lab-control single-ply and 4-ply P100/AZ91C/AZ61A laminates are shown in Figs. 14 to 16. Figs. 14 and 15 show that the behavior of both lab-control and post-flight LE was unstable, non-linear, had large, thermal hysteresis and residual strains. The post-flight LE shows better stability with smaller residual strain as compared to the lab-control. It is noted that, for both cases, the average length of the sample decreased with cycling. Again, however, the overall CTE was quite low and near-zero. The behavior of the Gr/Mg composites in this study is quite different from the results of other experiments (Refs. 2, 4, and 5). This observation again demonstrates that characterizing the thermal response of MMC can be complicated by secondary effects such as the processing procedure. Variations in the residual stresses existing in "as-fabricated" composites, for example, can have a dominant effect on the thermal response of MMC.

Figure 16 shows the response of 4-ply laminates over the same range of temperatures. It can be seen that the performances of multi-ply laminates differ considerably from the unidirectional single-ply composites. The 4-ply lab-control and LE samples show a closed thermal hysteresis loop with magnitude of about 100 μ-strain. The lab-control and post-flight samples have nearly identical curves. This indicates that the behavior of multi-ply laminates was originally quite stable, and extensive thermal cycling over the LDEF temperature range did not have much effect on their behavior over ±250°F. The thermal expansion was characteristically non-linear due to interply stresses. The total change in dimension was relatively small, about 50 μ-strain. The overall CTE is near-zero (0.071×10^{-6}/°F) over the test temperature range. Here again, as for the Gr/Al composites, the P100/AZ91C/AZ61A composites should also be evaluated post-flight over the LDEF temperature range. This will give a better indication of the stabilizing effect of the LDEF thermal cycling.

CONCLUSIONS

In this study, the thermal expansion behavior of MMC was fully evaluated to determine the synergistic effects of space environment such as high vacuum, solar radiation, atomic oxygen exposure, and micrometeoroid bombardment on these materials. The results obtained for these materials are very valuable for assessing their performance for space structures requiring low-CTE materials.

Gr/Al composites showed a stable, linear thermal expansion behavior with near-zero thermal hysteresis over the LDEF temperature range. Prolonged thermal cycling on LDEF also stabilized the thermal expansion of Gr/Al over wider temperature ranges. In contrast, Gr/Mg composites, even after extensive cycling during orbiting, showed non-linear, unstable behavior with significant hysteresis. However, the hysteresis was significantly reduced as compared to the as-fabricated samples. The thermal expansion data on Gr/Mg composites indicated that near-zero CTE over the application temperature range can be obtained and maintained on-orbit.

The flight data revealed that in the space environment, the temperature distribution in a structure is often time varying or non-uniform due to radiant heating. For a satellite like LDEF in a low earth orbit with alternating eclipse and sun exposure, the data showed that the materials experienced thermal cycling over different temperature extremes with different heating/cooling rates depending on the location of samples on the satellite. In a thermal cycle, the heating/cooling rates could vary from 0°F/min. to 20°F/min. when LDEF was going in or out of the earth's shadow. On the LE, the rates were almost double those on the TE. Two things were learned as a consequence of this phenomenon: first, the differential heating/cooling rates caused a difference in the total changes in dimension between LE and TE samples over the same temperature range as observed in Gr/Al composites, and second, thermal bending was observed on Gr/Mg composite materials due to their low thermal conductivity as compared to Gr/Al composites. The flight data also implied that structures in space are always subjected to non-uniform temperature distributions and thermal conductivity of a material is an important factor in establishing a uniform temperature distribution. Therefore, besides CTE and thermal hysteresis, thermal conductivity of a material must be considered to predict structural stability in the space environment. The application of Gr/Al composites offers advantages for space structures particularly where very tight thermal stability requirements in addition to high material performances are to be met. Gr/Al composites offer better thermal conductivity than Gr/Mg or Gr/Polymer composites, and also have lower susceptibility to space environmental effects as compared to Gr/Polymer composites (Refs. 6-8).

REFERENCES

1. G.L. Steckel and T.D. Le, "M0003-10: LDEF Advanced Composites Experiment" *LDEF First Post-Retrieval Symposium*, Kissimmee, FL, June 2-8, 1991, NASA CP-3134, pp. 1041-1053.

2. S.S. Tompkins, "Techniques for Measurement of the Thermal Expansion of Advanced Composite Materials" STP 1032, ASTM, Sparks, NV, 1988, pp.54-67.

3. E.G. Wolff and S.A. Eselun, "Double Michelson Interferometer for Contactless Thermal Expansion Measurement" *Proceeding of SPIE*, Vol. 192, Interferometry, 1979, pp. 204-208.

4. J.R. Strife and V.C. Nardone, "Thermal Expansion Behavior of Graphite Reinforced Metals" *Sixth Metal Matrix Composites Technology Conference*, Monterey, CA 1985, pp. 21-27.

5. K.W. Buesking, J.J. Kibler, B. Coffenberry, and C-F. Yen, "Advanced Composite Materials Evaluations" *MSC Technical Progress Report on NSWC*, Contract No. N60921-86-C-0236, Jan. 1987.

6. P.E. George and S.G. Hill, "Results from Analysis of Boeing Composite Specimens Flown on LDEF Experiment M0003," *LDEF First Post-Retrieval Symposium*, Kissimmee, FL, June 2-8, 1991, NASA CP-3134, pp. 1115-1141.

7. W.S. Slemp, P.R. Young, W.G. Witte, Jr., and J.Y. Shen, "Effects of LDEF Flight Exposure on Selected Polymer Matrix Resin Composite Materials," *LDEF First Post-Retrieval Symposium, Kissimmee*, FL, June 2-8, 1991, NASA CP-3134, pp. 1149-1162.

8. G.L. Steckel, T. Cookson, and C. Blair, "Polymer Matrix Composites on LDEF Experiments M0003-9 & 10," *Proceedings of LDEF Materials Workshops '91*, NASA CP-3162, pp. 515-542.

TABLE I

Aerospace Material Number	Material Description	Flight Data	Laser Interferometer Data
AL3-AL6	GY70/201/2024 (1 PLY)	LE & TE	LE, TE, and Lab-Control
AL12 & AL14	P55/6061/6061 (1 PLY)	LE & TE	LE, TE, and Lab-Control
AL33	P100/201/2024 (4 PLY/±20°S)		LE, TE, and Lab-Control
MG3 - MG6	P100/EZ33A/AZ31B (1 PLY)	LE & TE	LE, TE, and Lab-Control
MG9	P100/AZ91C/AZ61A (1 PLY)		LE and Lab-Control
MG10	P100/AZ91C/AZ61A (4 PLY/±10°S)		LE and Lab-Control

TABLE II

CTE of Gr/Al Composites (x 10^{-6}/°F)

Materials	Lab-Control	LE	TE
GY70/201/2024 (1 Ply)	3.5	3.2	3.8
P55/6061/6061 (1 Ply)	3.0	3.3	3.5

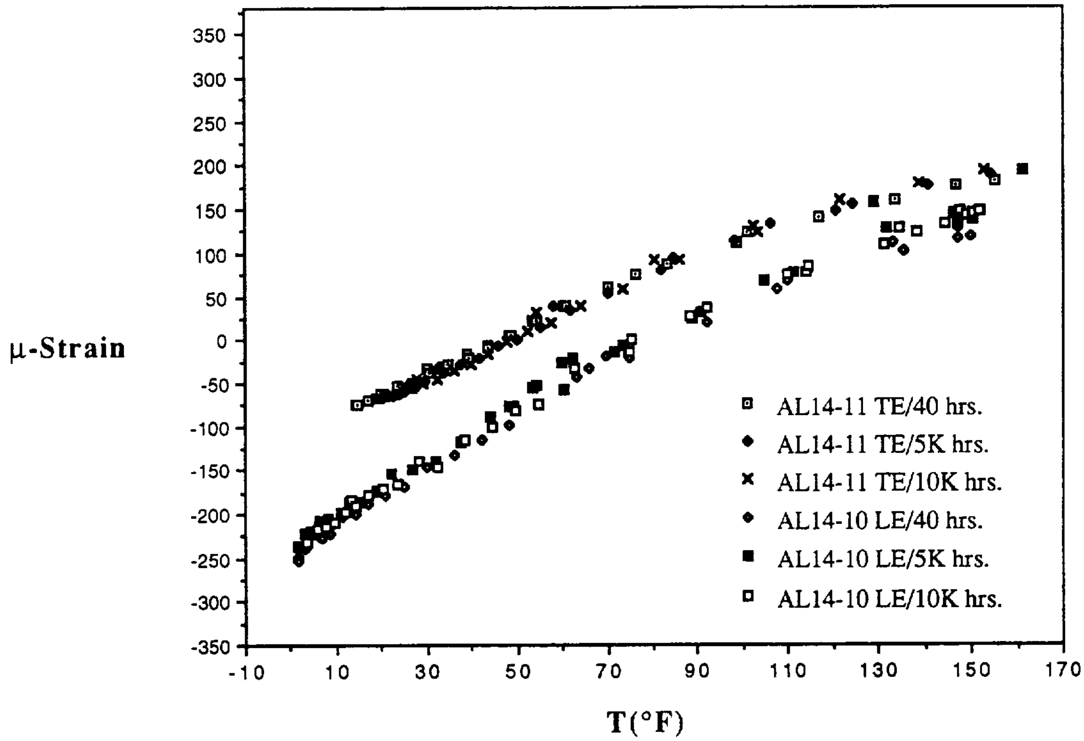

Fig. 1. Flight data showing the change in dimension vs. T of P55/6061/6061 Gr/Al composites

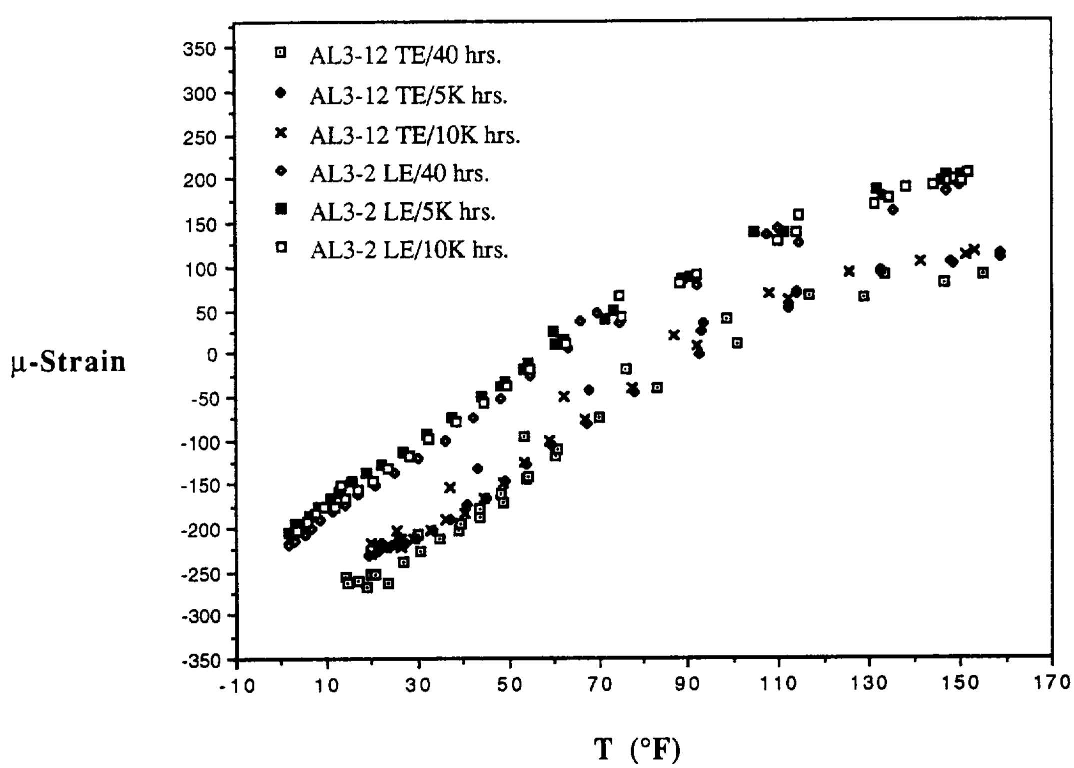

Fig. 2. Flight data showing the change in dimension vs. T of GY70/201/2024 Gr/Al composites.

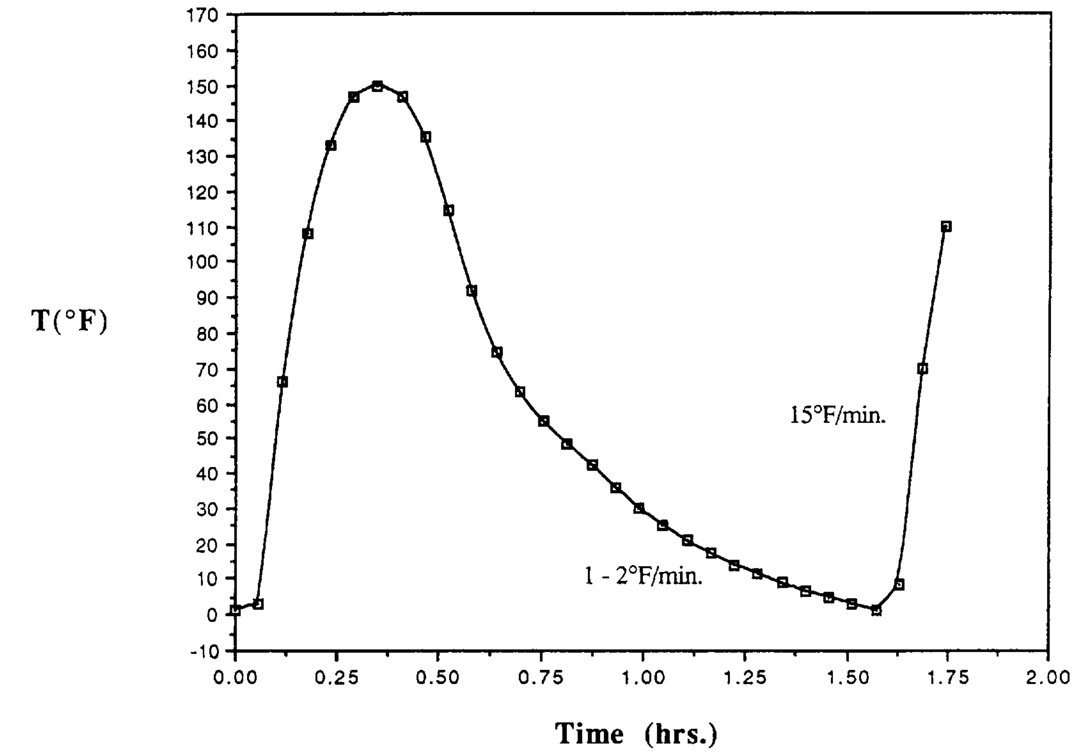

(a) LE

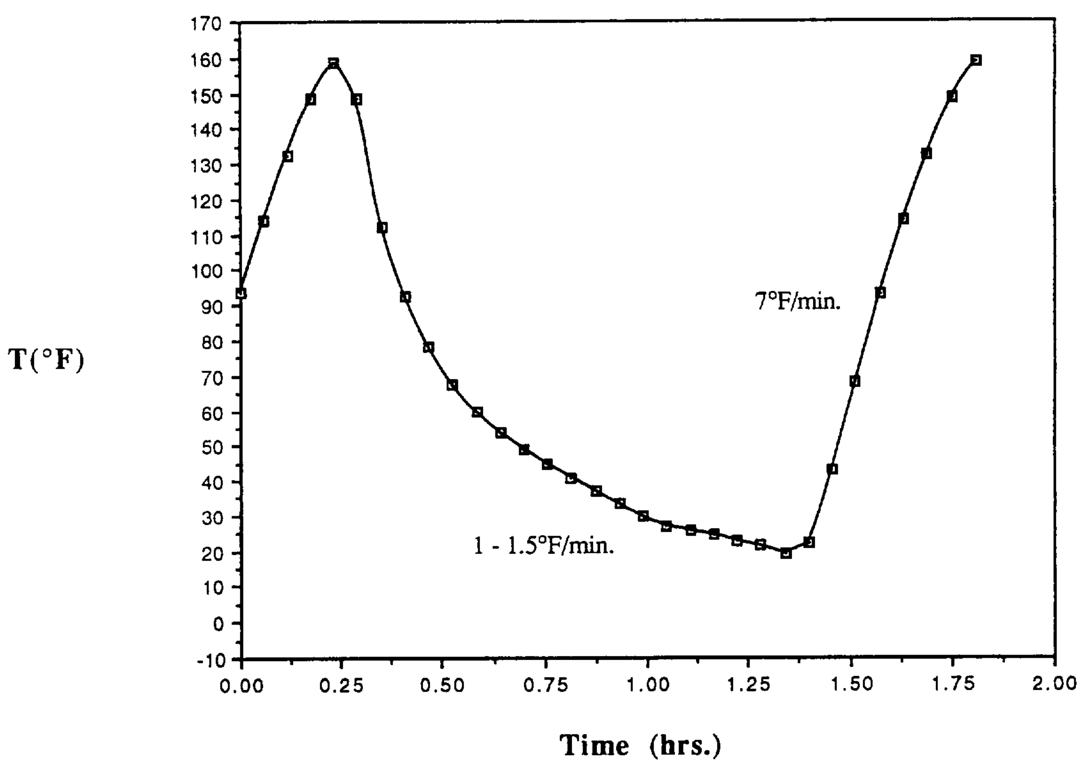

Fig. 3(b). TE

Fig. 3. Flight data showing the change in T vs. time in a single cycle of Gr/Al composites, (a) LE and (b) TE.

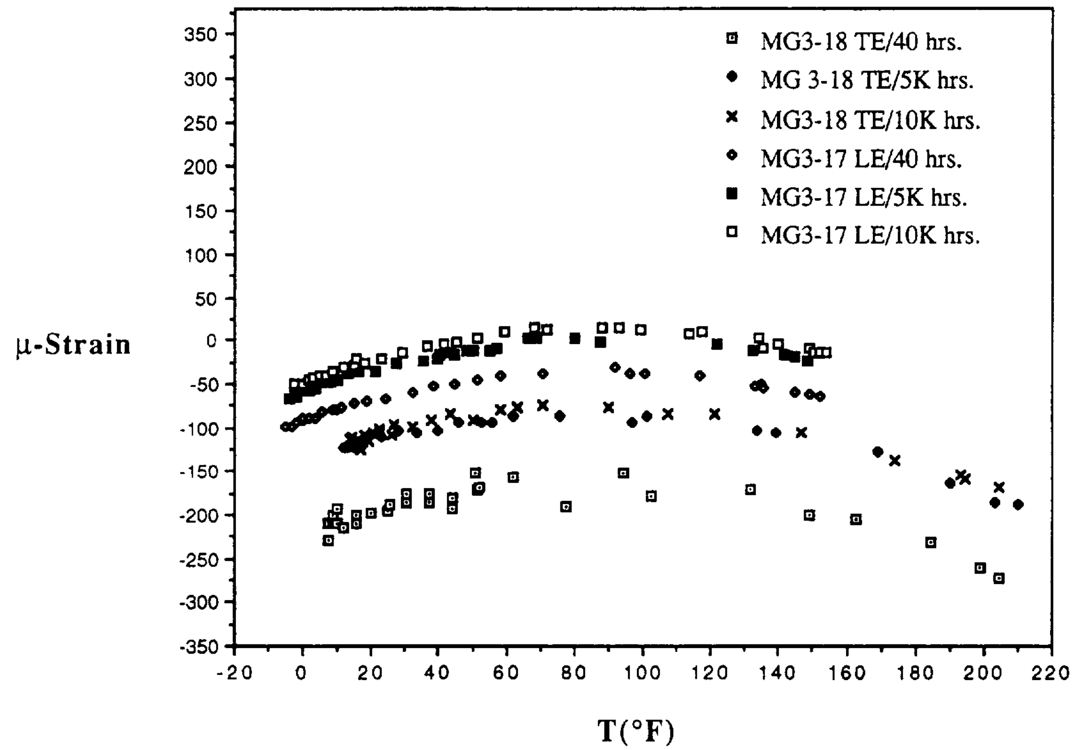

Fig. 4. Flight data showing the change in dimension vs. T of P100/EZ33A/AZ31B Gr/Mg composites.

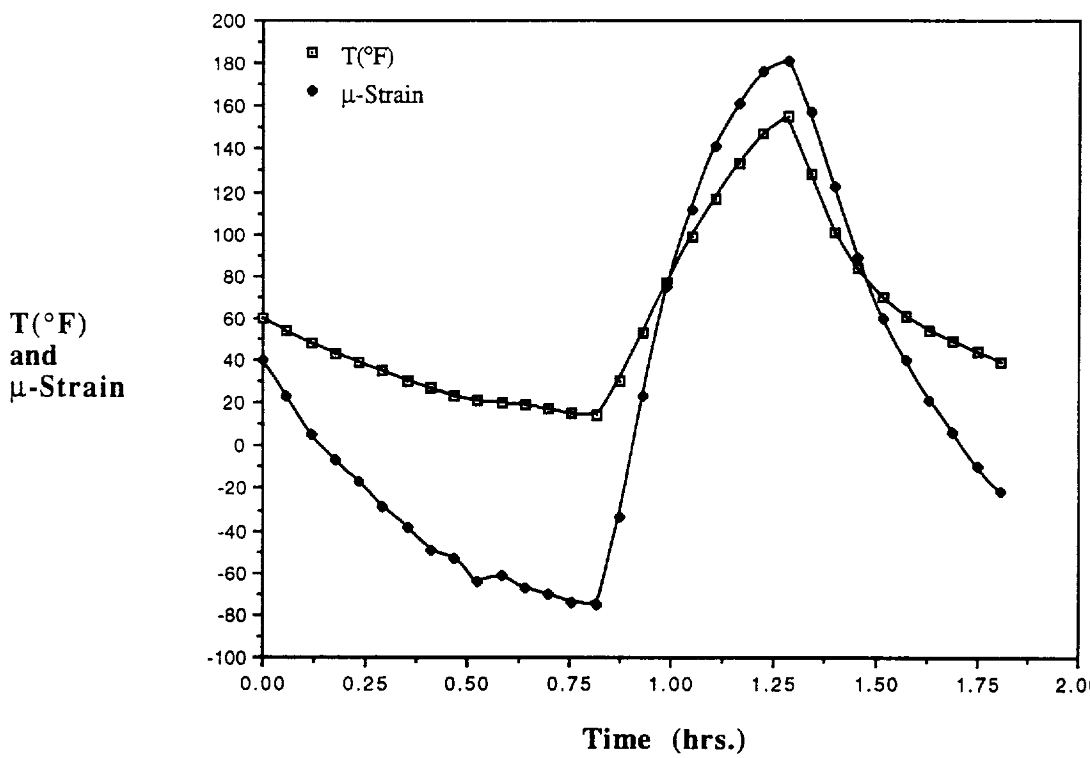

Fig. 5. Flight data showing the change in dimension and temperature vs. time in a thermal cycle of P55/6061/6061 composite.

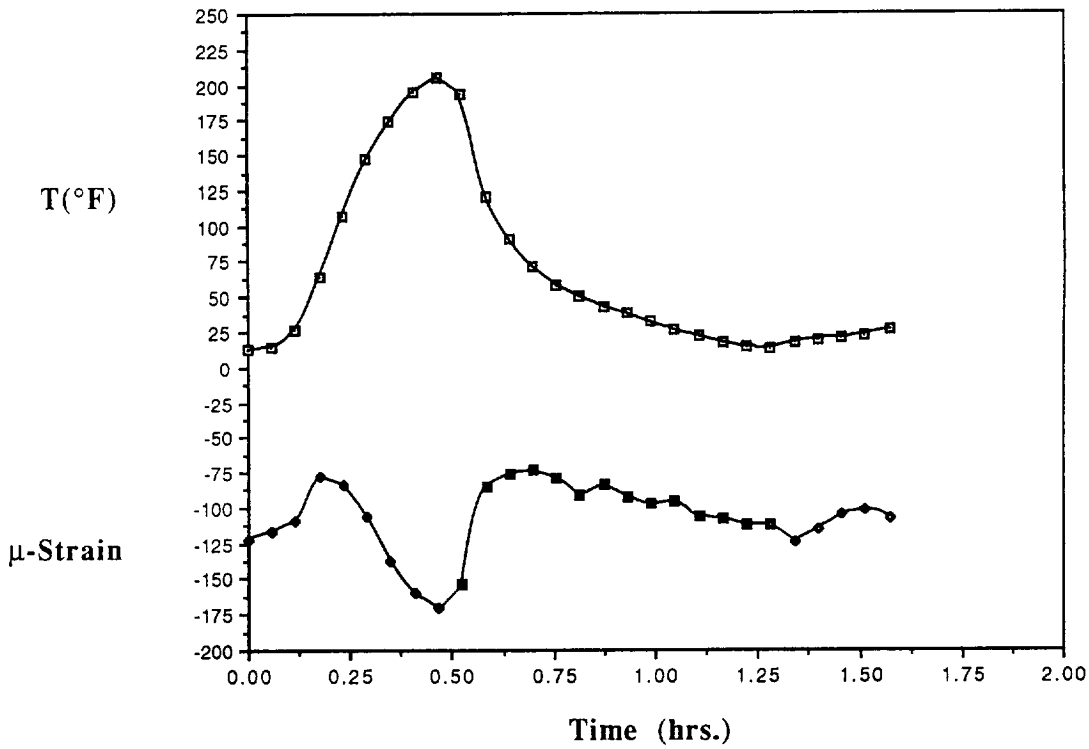

Fig. 6. Flight data showing the change in dimension and temperature vs. time in a single thermal cycle of P100/EZ33A/AZ31B Gr/Mg composites.

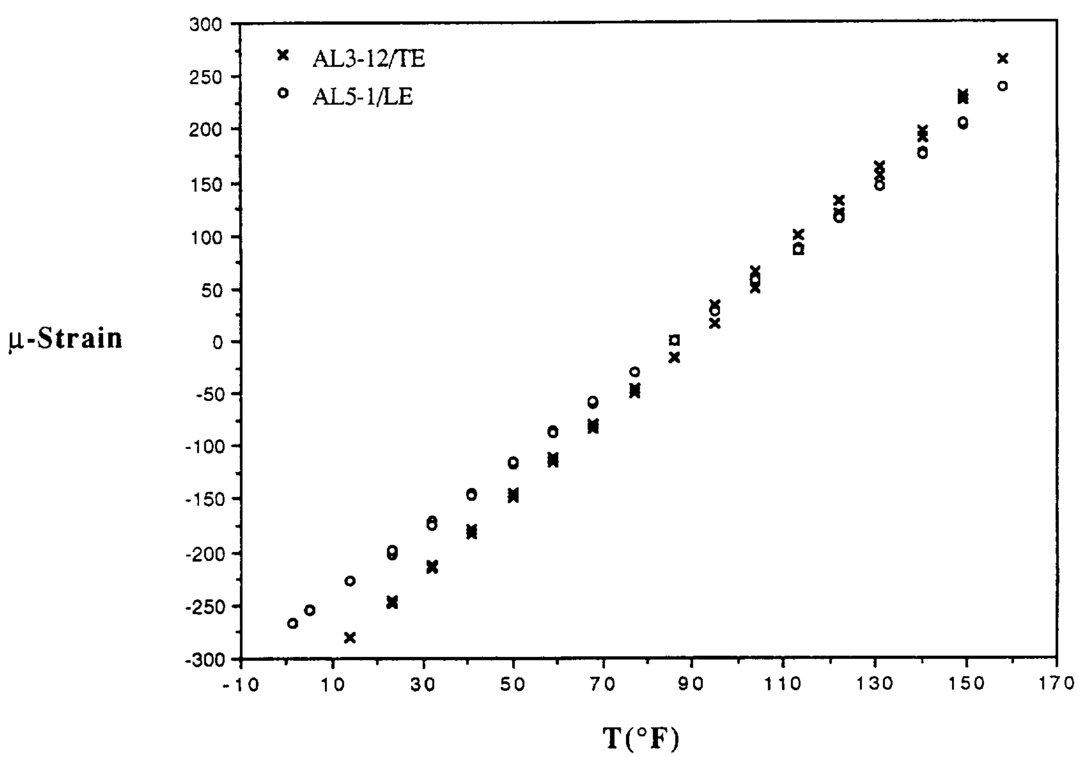

Fig. 7. Thermal expansion curves of the LE and TE sample of GY70/201/2024 Gr/Al composites determined by laser interferometry.

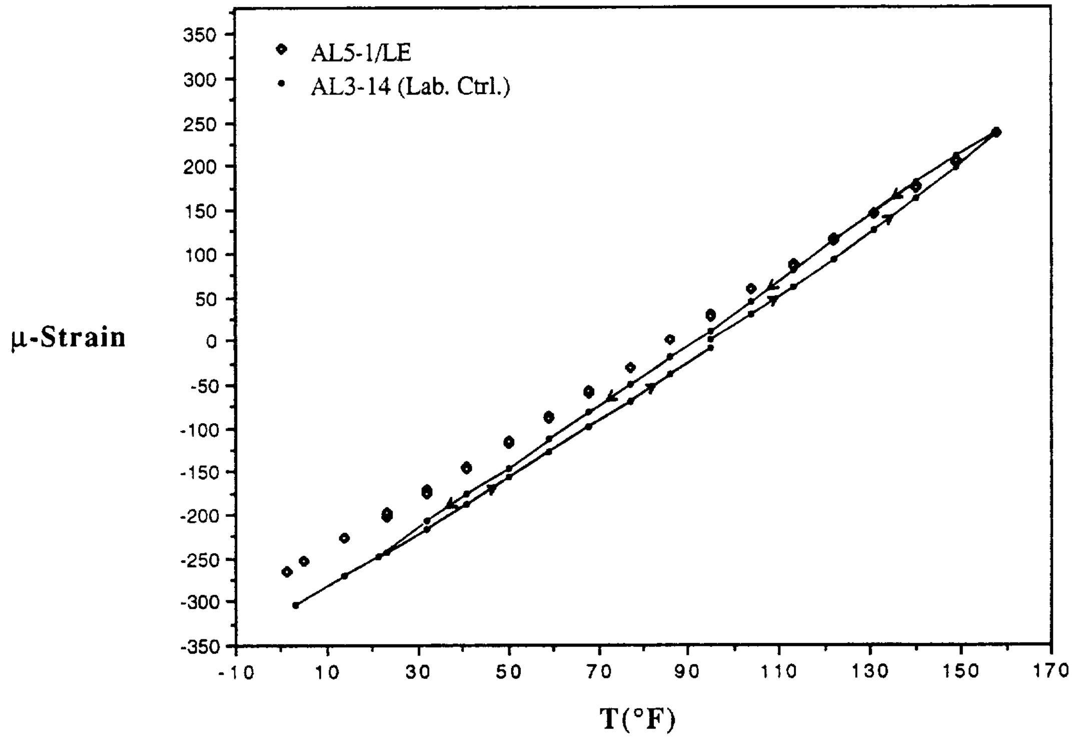

Fig. 8. Thermal expansion curves of lab. control and LE of GY70/201/2024 Gr/Al composites determined by laser interferometry.

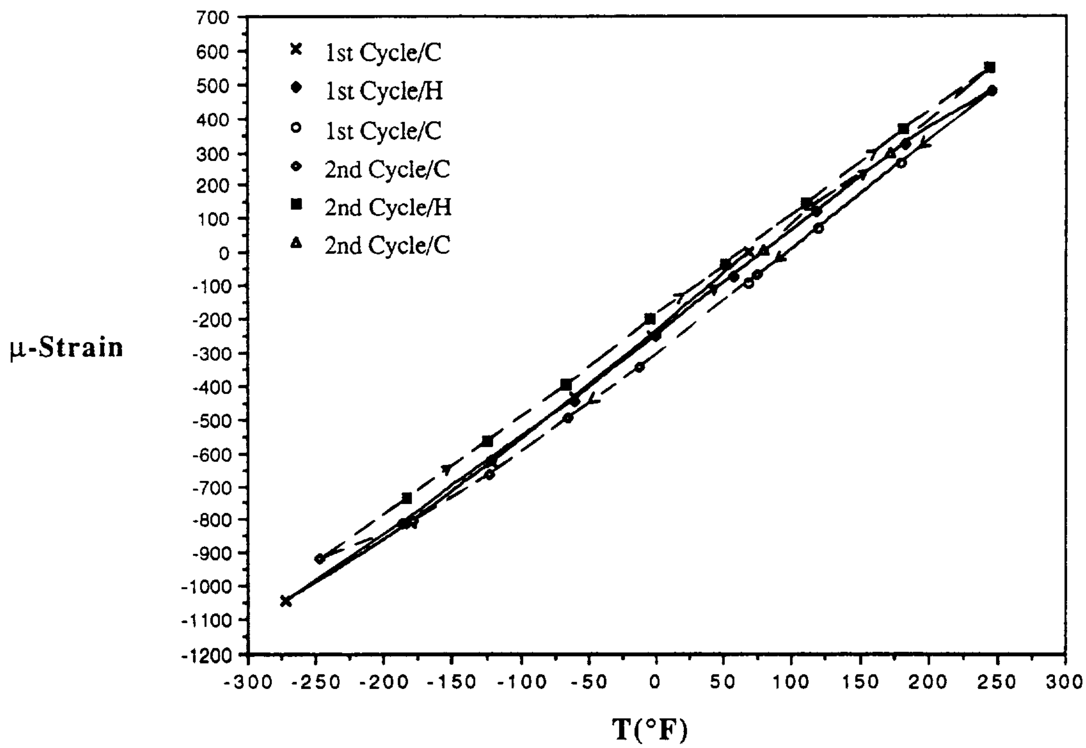

Fig. 9. Thermal expansion curves of the lab. control sample of GY70/201/2024 Gr/Al composites determined by laser interferometry.

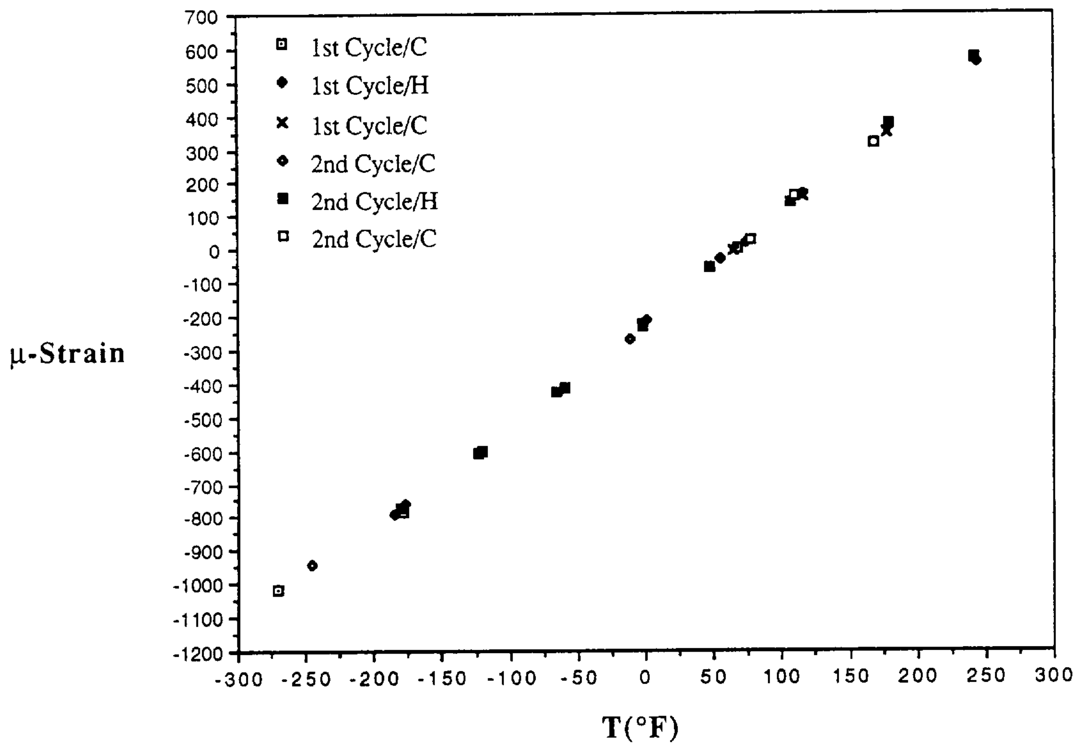

Fig. 10. Thermal expansion curves of the LE sample of GY70/201/2024 Gr/Al composites determined bv laser interferometrv.

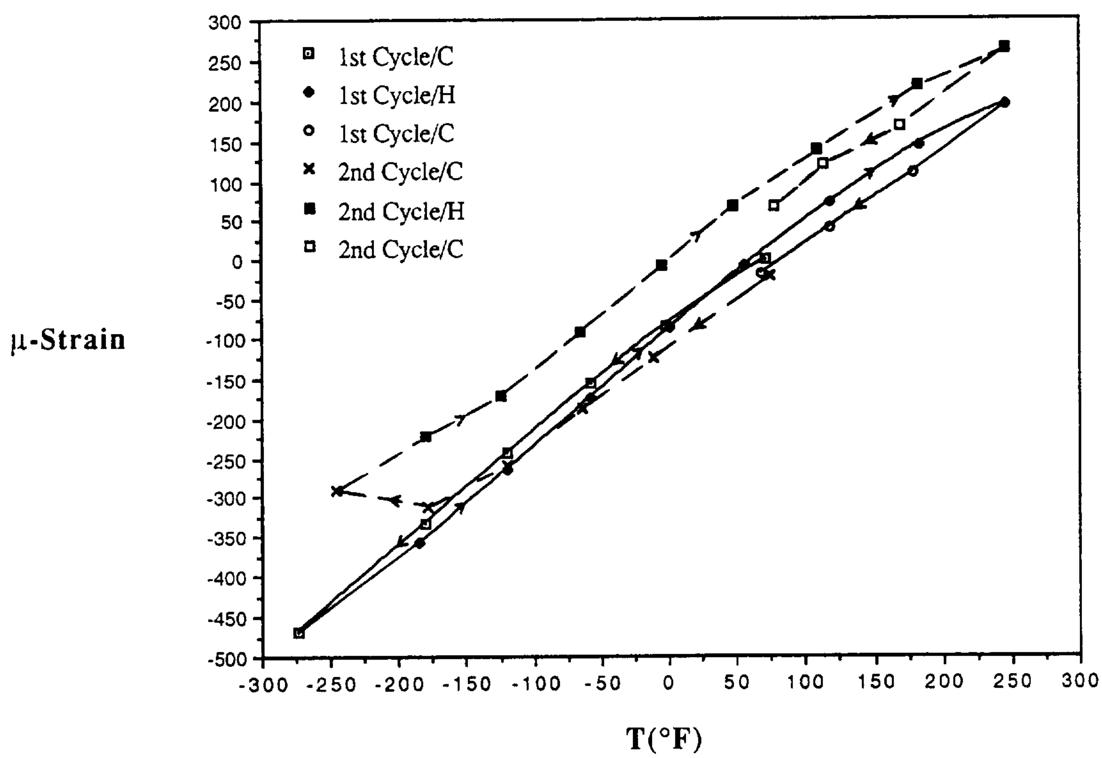

Fig. 11. Thermal expansion curves of the lab. control sample of P100/201/2024 (4-ply) Gr/Al composites determined by laser interferometry.

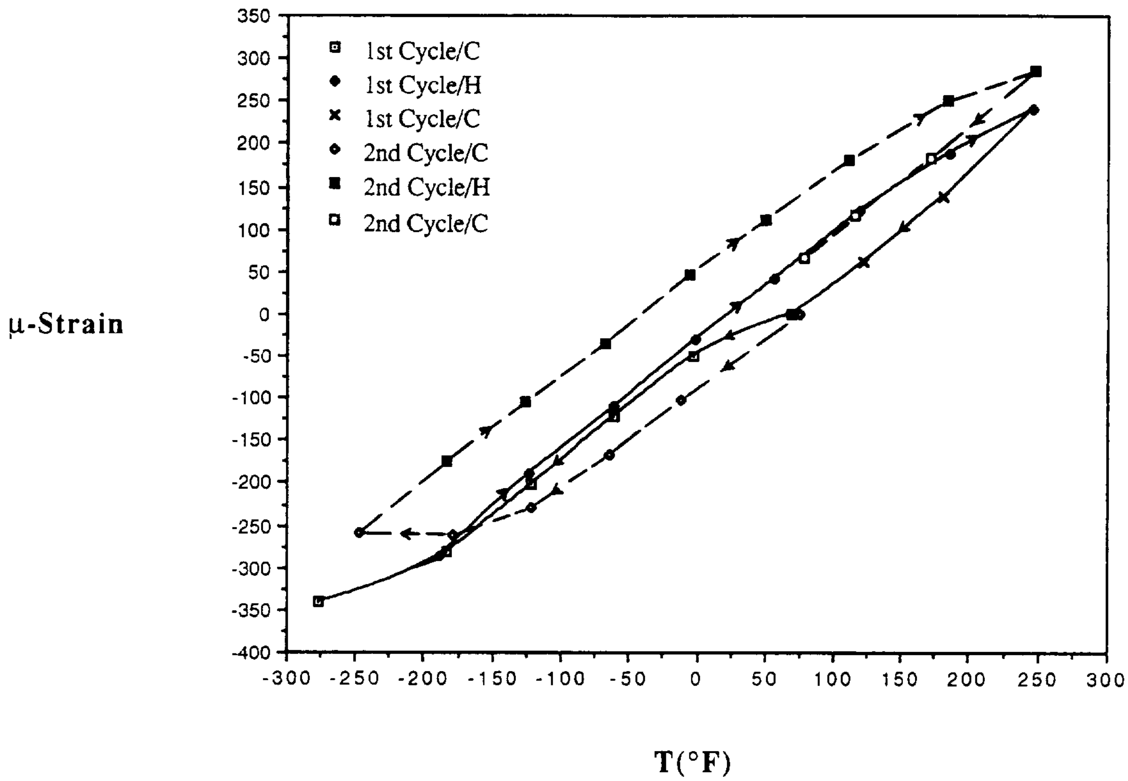

Fig. 12. Thermal expansion curves of the LE sample of P100/201/2024 (4 ply) Gr/Al composites determined by laser interferometry.

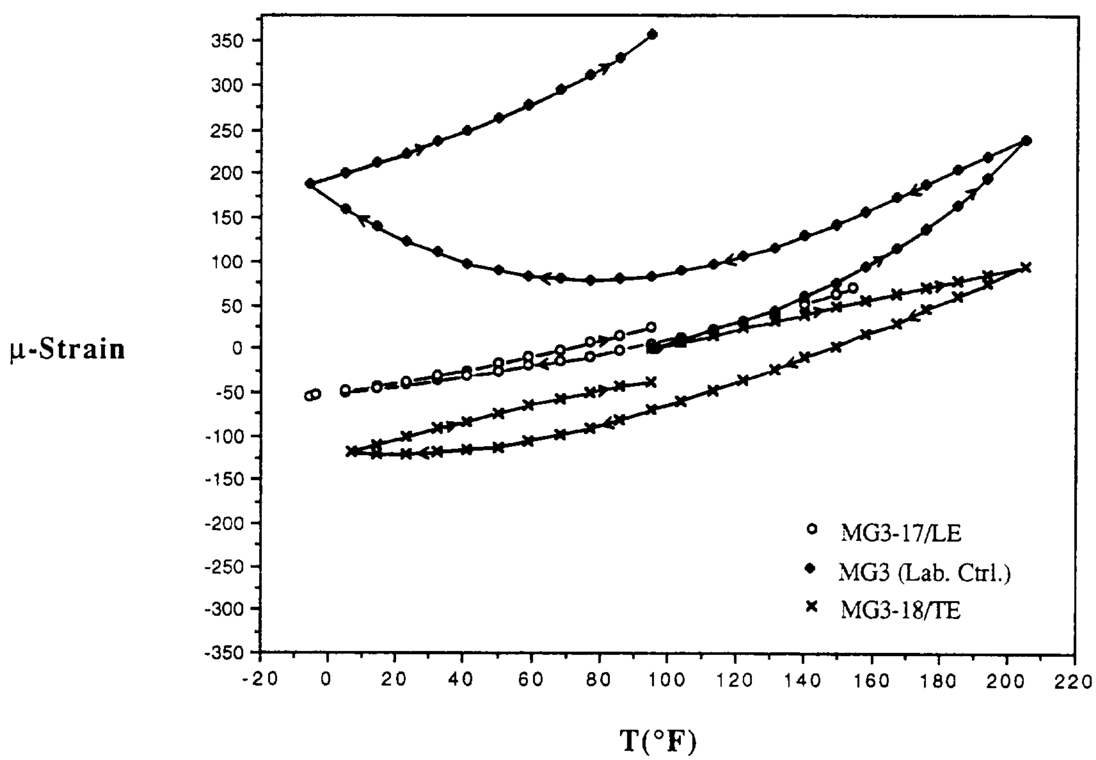

Fig. 13. Thermal expansion curves of the LE, TE, and lab. control sample of P100/EZ33A/AZ31B Gr/Mg composites determined by laser interferometry.

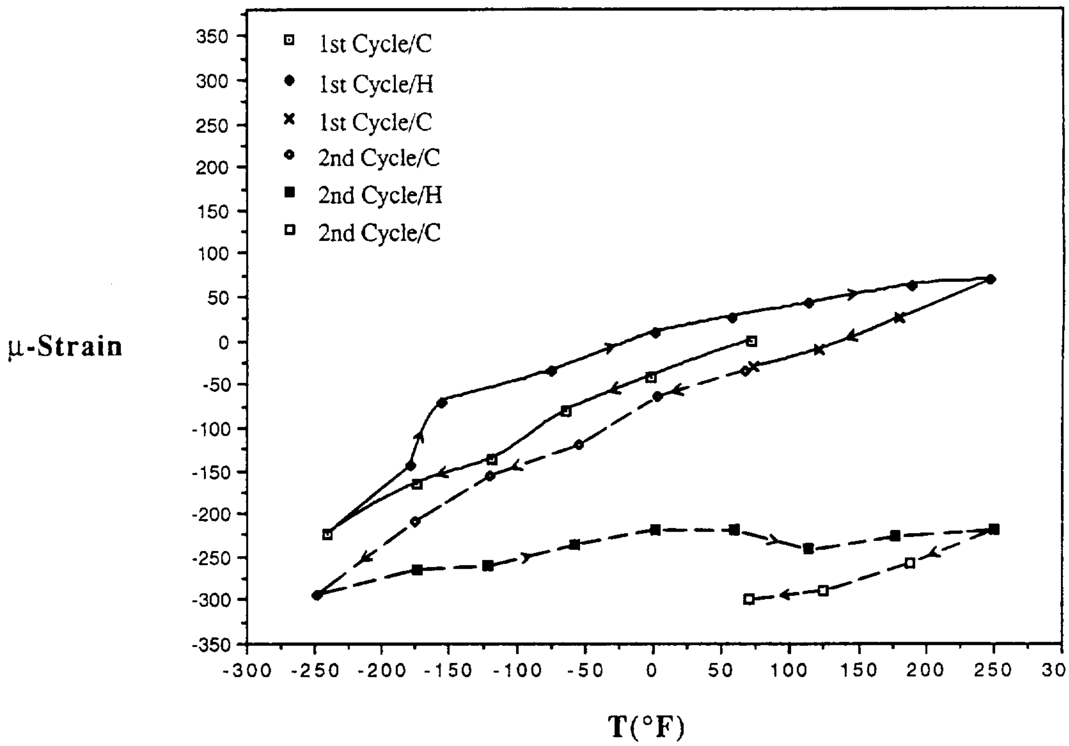

Fig. 14. Thermal expansion curves of the lab. control sample of P100/AZ91C/AZ61A Gr/Mg composites determined by laser interferometry.

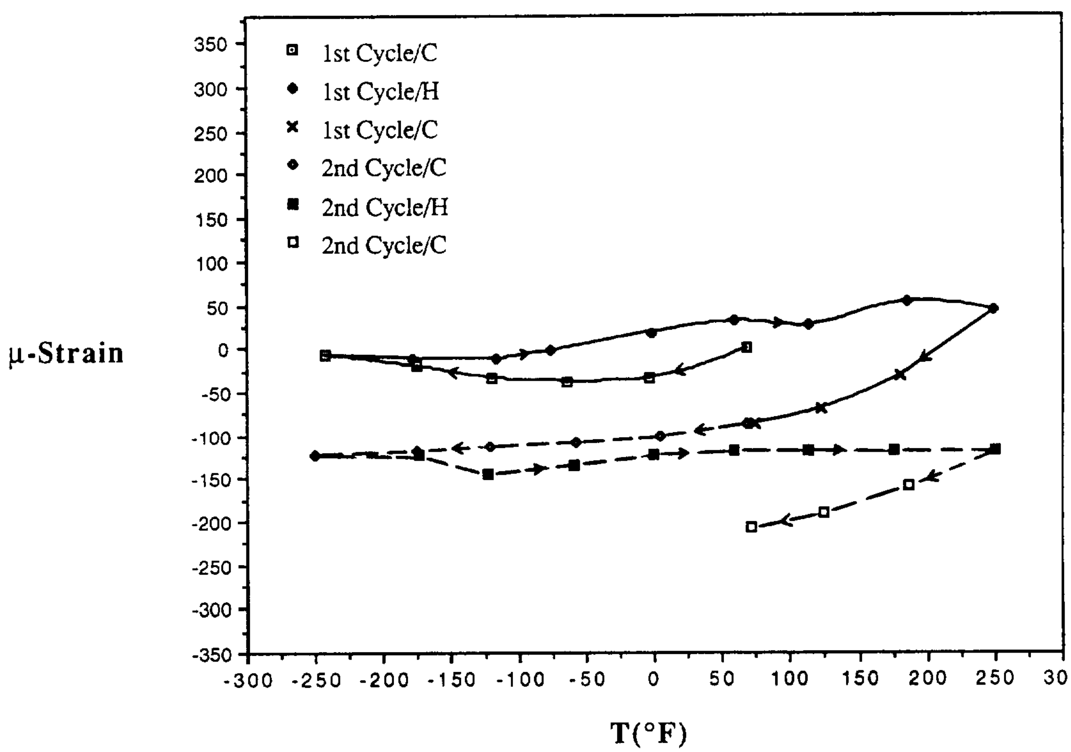

Fig. 15. Thermal expansion curves of the LE sample of P100/AZ91C/AZ61A Gr/Mg composites determined by laser interferometry.

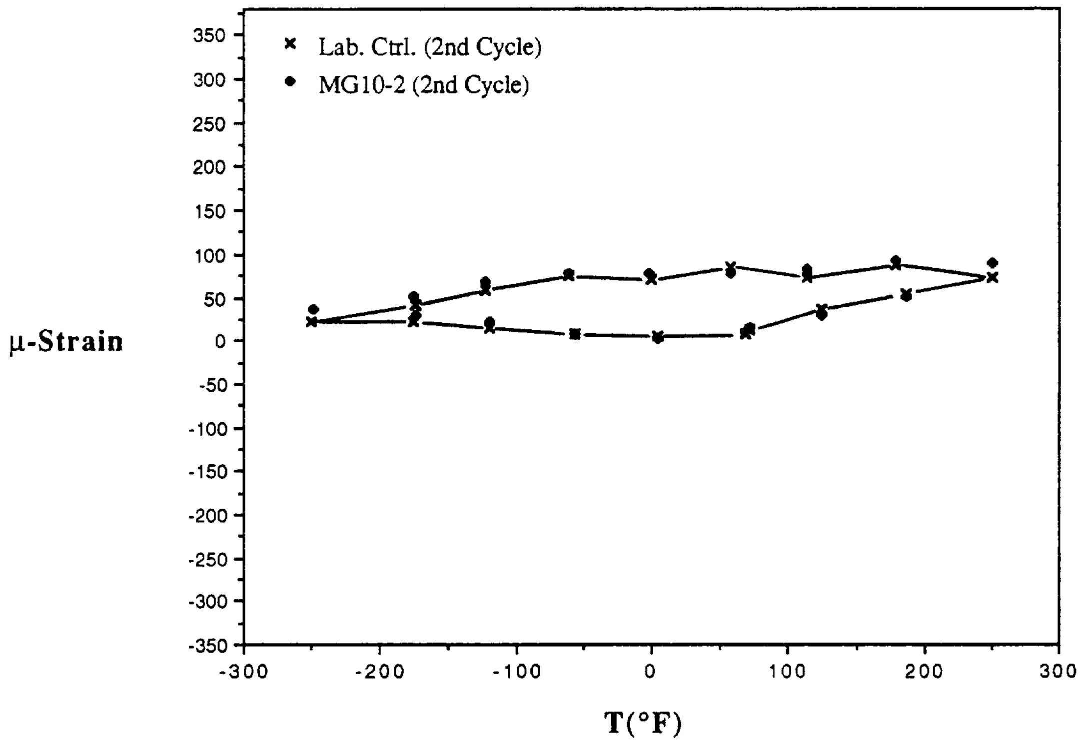

Fig. 16. Thermal expansion curves of the lab. control and LE sample of P100/AZ91C/AZ61A (4 ply) Gr/Mg composites determined by laser interferometry.